Cell Proliferation

Cell Prolif., 2012, **45**, 445–455 doi: 10.1111/j.1365-2184.2012.00835.x

Mathematical model of heterogeneous cancer growth with an autocrine signalling pathway

G.-M. Hu*, C.-Y. Lee*, Y.-Y. Chen†, N.-N. Pang* and W. J. Tzeng‡

*Physics Department, National Taiwan University, Taipei, Taiwan, †National Center for Theoretical Sciences, Physics Department, Institute of Astrophysics, National Taiwan University, Taipei, Taiwan and ‡Physics Department, Tamkang University, New Taipei City, Taiwan

Received 18 November 2011; revision accepted 20 April 2012

Abstract

Objectives: Cancer is a complex biological occurrence which is difficult to describe clearly and explain its growth development. As such, novel concepts, such as of heterogeneity and signalling pathways, grow exponentially and many mathematical models accommodating the latest knowledge have been proposed. Here, we present a simple mathematical model that exhibits many characteristics of experimental data, using prostate carcinoma cell spheroids under treatment.

Materials and methods: We have modelled cancer as a two-subpopulation system, with one subpopulation representing a cancer stem cell state, and the other a normal cancer cell state. As a first approximation, these follow a logistical growth model with self and competing capacities, but they can transform into each other by using an autocrine signalling pathway.

Results and conclusion: By analysing regulation behaviour of each of the system parameters, we show that the model exhibits many characteristics of actual cancer growth curves. Features reproduced in this model include delayed phase of evolving cancer under 17AAG treatment, and bi-stable behaviour under treatment by irradiation. In addition, our interpretation of the system parameters corresponds well with known facts involving 17AAG treatment. This model may thus provide insight into some of the mechanisms behind cancer.

Correspondence: G.-M. Hu, Physics Department, National Taiwan ?University, No. 1, Sec. 4. Roosevelt Road, Taipei 106, Taiwan. Tel.: +886- 918-173-326; Fax: +886-2-2363-9984; E-mail: pipipshu@gmail.com

Introduction

Cancer, a disease of a group of abnormal cells with largely uncontrolled proliferation, is still one of the main lethal diseases of modern human societies. Concerning its origin, no consensus has yet been reached, although the cancer stem-cell hypothesis is gaining popularity (1); this assumes that a malignant system with epigenetic heterogeneity has at least one subpopulation with high proliferation ability. In addition to this are recent discussions that different subpopulations in cancer may transform into other subpopulations as a result of autocrine signalling pathways (2,3). In this regard, these subpopulations thus may be treated as different phenotypes of the cancer cells. Taken at face value, this implies that one may be able to view cancer as a classical population dynamic system of at least two variables, with each variable representing a population of a species interacting with other species in the system.

In view of the fact that a systemic mathematical model of a carcinoma cell group can help us better understand the cancer system (4), several mathematical models have been proposed (5). For example, Garner *et al.* proposed a two-subpopulation model, with one proliferation and one quiescent subpopulation, with transition potential (6). Ganguly and Puri constructed a mathematical model on regulation of signalling pathways with mutations based on the cancer stem-cell hypothesis (7). Recently, the transition effect between heterogeneous subpopulations of a tumour due to auto/para-crine signalling pathways, has been discussed (2,3). Mathematical models on tumourigenesis with auto/para-crine signalling pathway effects have also been proposed. For example, Bajzer and Vuk-Pavlović proposed a population model in which a single species of cells can interact under certain growth stimulation activity (8), and Ghosh *et al.* further discussed a model allowing spatial variation (9). In addition, a mathematical model used to interpret or even provide guidance for experimental data of cancer treatment, has also become a lively discussed topic (10–13).

In this article, we present a simple two-subpopulation mathematical model with logistic growth mode and transition effects due to an autocrine signalling pathway. To compare this with actual experimental data, we have also modelled the process of therapy phenomenologically, with some of the system parameters. We show that numerical results can be brought into correspondence with a series of real tumour growth curves of prostate carcinoma spheroids, treated with 17-*N*-allylamino-17-demethoxy geldanamycin and acute irradiation, performed by Enmon *et al.* (14). Specifically, characteristics such as presence of a delay phase and bi-stable behaviour, are manifest in some parameter regimes of the model.

The mathematical model

Figure 1 conveys the concept schematic of our model. It is a two-subpopulation model, with x_1 being the population of the normal cancer cell state and x_2, the population of the cancer stem cell state. To simplify the mathematics while at the same time capturing the essence of what may be causing the observed behaviour, we deliberately assigned the same proliferation rate r to both states, leaving the more general case for later study. Due to competition of cells in the same cell state, x_1 has a logistic suppressing capacity, C_1. We assume that x_1 and x_2 are also competing with each other, and the 'suppressing capacity' of x_2 on x_1 is C_2 (Roughly, this means that suppression from x_2 on x_1 becomes important when x_2 grows to a value which is of the same order of magnitude of C_2). If we would like state 1 to quickly experience suppression from state 2 during the growth process, then we will have to assume $C_1 >> C_2$, which is precisely what we will adopt in the present model. Self-suppressing capacity of x_2 is aC_2, with a being the 'heterogeneity coefficient'. As we have taken state 2 to be the cancer stem cell state, it must have a larger self-suppressing capacity. We thus assume in our model that $a >> 1$ in such a way that $aC_2 >> C_1$. For simplicity, we also assume that suppressing capacity of x_1 on x_2 is aC_1. For convenience, variable and parameter setting of our model is summarized in Table 1.

General mathematical form of the logistic growth and competition model under an autocrine signalling pathway, is assumed to take the form

$$\begin{cases} \dot{x}_1 = r\left(1 - \left(\frac{x_1}{C_1} + \frac{x_2}{C_2}\right)\right)x_1 - k_{12}w_2x_1 + k_{21}w_1x_2, \\ \dot{x}_2 = r\left(1 - \frac{1}{a}\left(\frac{x_1}{C_1} + \frac{x_2}{C_2}\right)\right)x_2 + k_{12}w_2x_1 - k_{21}w_1x_2, \end{cases} \tag{1}$$

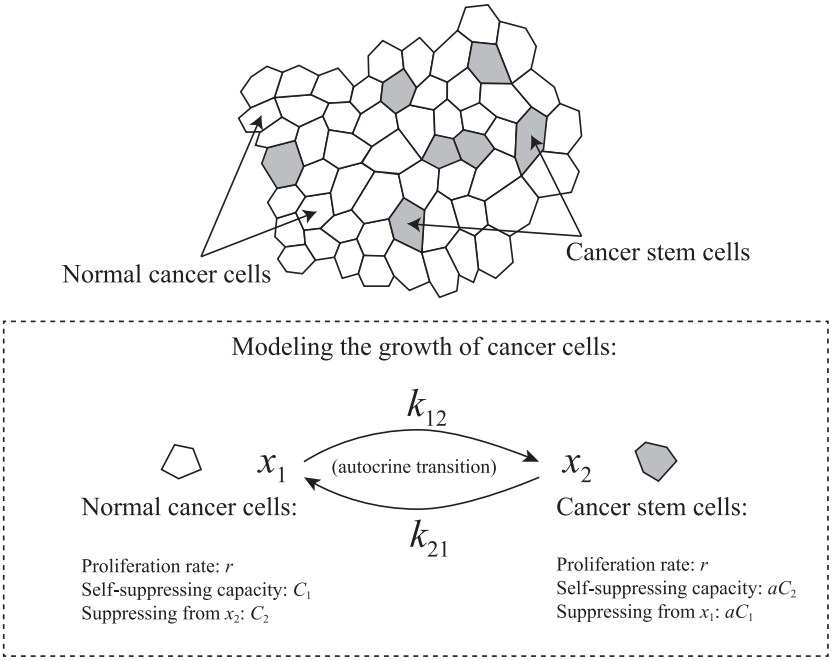

Figure 1. Schematic of the two-subpopulation tumour model with transition due to auto/para-crine signalling pathway. x_1 and x_2 are the two subpopulations in a cancer system each of which follows the logistic growth mode with proliferation r. x_1 has a self-suppressing capacity C_1. The growth of x_1 is also suppressed by x_2 due to competition. This is characterized by extra suppressing capacity C_2 of x_2 on x_1. Heterogeneity coefficient a introduces asymmetry between the two states: State 2 has a self-suppressing capacity aC_2, and a corresponding suppressing capacity aC_1 from state 1. These two subpopulations have a transition effect due to autocrine signalling pathways. The strength of the autocrine effect from x_1 to x_2 is k_{12}, and k_{21} is that of x_2 to x_1.

Table 1. Variables and parameters used in general growth and transition model

Variables and parameters	Symbols
Population of normal cancer cells	x_1
Population of cancer stem cells	x_2
Total population of the cancer system	x_t
Weighting of x_1	w_1
Weighting of x_2	w_2
Proliferation rate x_1	r
Proliferation rate x_2	r
Self carrying capacity x_1	C_1
Suppressing capacity of x_2 on x_1	C_2
Heterogeneity coefficient	a
Autocrine strength of x_1 to x_2	k_{12}
Autocrine strength of x_2 to x_1	k_{21}

where $w_i \equiv \frac{x_i}{x_1+x_2}$ is weighting of the *i*-th subpopulation. In the above, the mathematical form of the autocrine signalling pathway follows that suggested by Chang *et al.* (15), for the stem cell model. The autocrine form w_2x_1 or w_1x_2 means that an individual would change into the other state with a probability proportional to the percentage of the other state in the system. Clearly, this can be viewed as one kind of mean field effect of the autocrine signalling pathway. Also, k_{12} is the autocrine transition rate strength of x_1 to x_2, and k_{21} is that of x_2 to x_1. We chose to adopt this form from the work of Ref. (15) for two reasons: (i) it conveys the very idea of how a cell state can transform into another in a mathematically succinct manner and (ii) non-linearity introduced by these authors is not so overly complicated as to render analytical treatments impossible in our model.

As the term modelling the autocrine signalling pathway from x_1 to x_2 and from x_2 to x_1 is the same, that is, $w_2x_1 = w_1x_2 = \frac{x_1x_2}{x_t}$, we can follow Chang *et al.* (15) to set an autocrine strength coefficient $k \equiv k_{21} - k_{12}$ to substitute for the two coefficients k_{12} and k_{21}, where $x_t \equiv x_1 + x_2$. Then, growth and transition equations become

$$\begin{cases} \dot{x}_1 = r\left(1 - \left(\frac{x_1}{C_1} + \frac{x_2}{C_2}\right)\right)x_1 + k\frac{x_1x_2}{x_t}, \\ \dot{x}_2 = r\left(1 - \frac{1}{a}\left(\frac{x_1}{C_1} + \frac{x_2}{C_2}\right)\right)x_2 - k\frac{x_1x_2}{x_t}. \end{cases} \quad (2)$$

To facilitate comparison of our model with experimental data, it is more convenient to change the variables from (x_1, x_2) to $(x_t \equiv x_1 + x_2, w_1 \equiv \frac{x_1}{x_t})$. Transformed equations read (see Appendix A for the derivation)

$$\begin{cases} \dot{x}_t = rx_t\left(1 - \left[\left(w_1 + \frac{1-w_1}{a}\right)\left(\frac{w_1}{C_1} + \frac{1-w_1}{C_2}\right)\right]x_t\right), \\ \dot{w}_1 = k\left\{1 - \frac{r}{k}\left(1 - \frac{1}{a}\right)\left(\frac{w_1}{C_1} + \frac{1-w_1}{C_2}\right)x_t\right\}(w_1 - w_1^2). \end{cases} \quad (3)$$

Listed in Table 2 are the numerical values we have adopted for our model, when a cancer system has not received any treatment. Later, we will investigate how the parameters can be modified to better fit growth curve data of prostate carcinoma spheroids, with treatment discussed by Enmon *et al.* (14).

Results and discussion

Some simple properties of this model

As we have adopted a simple model, interpretation of each of its system parameters becomes more transparent. For example, the reciprocal of r is the characteristic time of the system, and it determines duration of the total growth period. Larger r clearly corresponds to shorter growth time. But from the mathematical point of view, r can always be absorbed into the time so that its absolute value will not really concern us.

A simple analysis shows that the autocrine parameter k can be used to regulate final dominant state (see Appendix C). When $k > (a - 1)r$, species 1 dominates the final scene, whereas the opposite is true, if $k\left(1 - \frac{1}{a}\right)r$. (This should appear plausible with a view of eqn 2 if we consider the limiting cases $k \to \infty$ and $k \to 0$.) But for an intermediate value of k, that is, when $\left(1 - \frac{1}{a}\right)rk(a-1)r$, the system goes into a bi-stable situation, with the final state being dominated by either x_1 or x_2, depending on initial conditions. With all other parameters fixed, Fig. 2 shows a series of growth curves for different values of k. Here, we see that final size of x_t is 10^4, which is the self-suppressing capacity of x_1, when $k = 10$ (In this sense, k can be considered to be large in this parameter regime). But when we tune k to a lower value, the transition effect may switch the final dominant state, depending on initial values. If we fix the initial value of w_1 and tune initial total population x_t, then x_2 will eventually dominate if $x_t(0)$ is larger than a certain critical initial size. Value of the critical size depends on strength of k in a reciprocal manner: critical size increases when k decreases (This can be better seen by looking at the terms inside the curly brackets of eqn 3). As $k(1 - \frac{1}{a})r$, final dominant state is always x_2.

Table 2. Parameter values of the cancer system without treatment

Parameters	Symbols	Values	Units
Proliferation rate of x_1 and x_2	r	0.3	1/day
Self carrying capacity of x_1	C_1	10^4	μm^3
Suppressing capacity of x_2 on x_1	C_2	2	μm^3
Heterogeneity coefficient	a	10^6	None
Autocrine strength	k	2.5	1/day

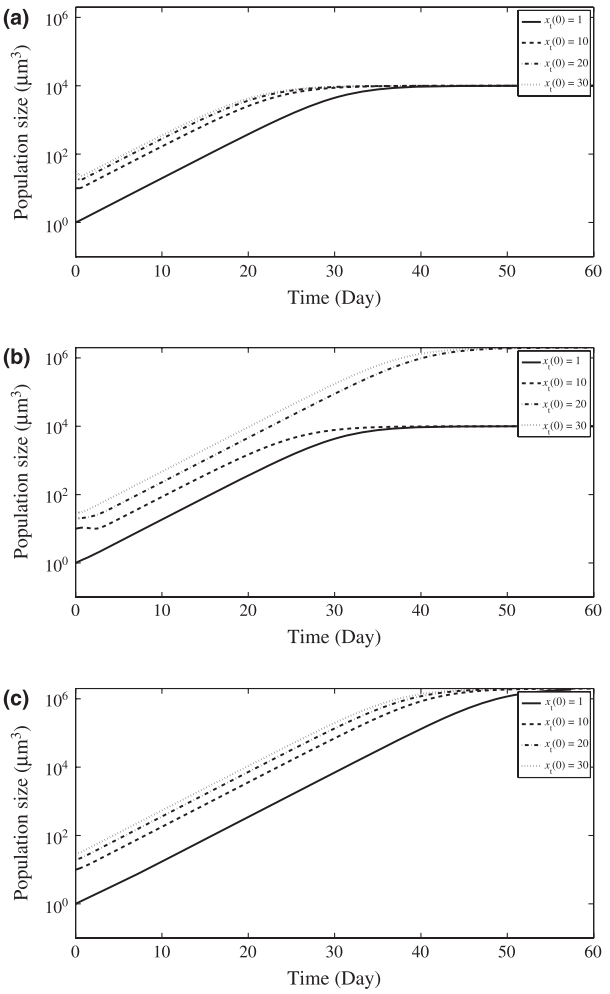

Figure 2. A demonstration that autocrine parameter k can regulate the dominant state and the bi-stable behavior. Series of x_t growth curves with fixed system parameters ($r = 0.3$, $a = 10^6$, $C_1 = 10^4$, $C_2 = 2$) and initial conditions ($x_t(0) = 1, 10, 20, 30$; $w_1(0) = 0.1$), but with different k. (a) $k = 10\left(1 - \frac{1}{a}\right)r$: all curves saturate at 10^4, self-suppressing capacity of x_1, meaning state 1 eventually dominates. (b) $k = 2.5$: As k becomes smaller, the final state of each growth curve depends on the size of the total initial population $x_t(0)$. Species 1 dominates for small $x_t(0)$; but state 2 dominates when $x_t(0)$ exceeds a certain critical size (growth curves all saturate at 10^6). (c) As k becomes much smaller ($k = 0.1$), critical $x_t(0)$ size is also larger. When k is large enough, the critical size no longer exists and state 2 dominates the final scene.

By our construction, $C_1 >> C_2$, so that typically, terms in eqn 3 involving C_1 can be ignored when compared to those containing C_2; also, with regard to the role played by the suppressing capacity C_2, we may say that it provides us with a mechanism to exhibit a 'delay' feature that might exist between initial growth stage and final settling state. This is so because C_2 acts to suppress growth of species 1, and whenever species 1 is destined to be the final dominant population, C_2 will simply act to fight against that unavoidable trend. This is particularly true when C_2 is small, as then a small population of species 2 is enough to effectively inhibit initial growth of species 1. Therefore, it will take a longer time for species 1 to grow to a significant percentage in the population (*via* the autocrine parameter k) before the suppressing effect from species 2 can be quenched (at a later time, the effect of C_2 diminishes simply because the population of species 2 is reduced, again, by the autocrine parameter k). All this is reflected in duration of time evolution before the system eventually settles. Detailed analysis of this aspect is provided in Appendix B, together with an approximate mathematical form of this property presented in Appendix D. In Fig. 3, we show growth curves for various values of C_2 when all other parameters and initial values are fixed. Once again, we note that the delay is more pronounced when C_2 is small.

Finally, we notice that the heterogeneity coefficient a is the key factor deciding which species is the proliferation state. When $a > 1$, x_2 is the proliferating subpopulation, and the reverse is true when $a < 1$. This is obvious as we have constructed our model so that the roles of x_1 and x_2 are exchanged when a is replaced by $1/a$. However, if we insist on adopting the same parameter regimes for other system parameters, but simply allow a to be less than unity, then delayed evolution, such as described above, is *not* expected to occur as now the associated suppressing capacity of species 1 on species 2 (as characterized by the coefficient aC_1) is not small.

Comparison of numerical results and real data from tumour growth, with treatment

By associating our system parameters with the various different aspects related to medical treatment for cancer, we are able to fit our numerical results with the experimental data of prostate carcinoma spheroids with treatment with 17-*N*-allylamino-17-demethoxy geldanamycin, and acute irradiation (14); below, we discuss such possibilities.

17AAG

17-*N*-allylamino-17-demethoxy-geldanamycin (17AAG), a geldanamycin analogue, can inhibit activity of heat shock protein 90, which may provide a mechanism to evade apoptosis of tumour cells (16). As 17AAG can inhibit evading the apoptotic mechanism of tumour cells, we can naturally associate it with one of the capacity parameters of our model. Specifically, a cancer system receiving this treatment might correspond to having a smaller value of C_2. From comparison with the actual treatment data of Ref. (14) and our numerical results, we found that dosage concentration of 17AAG and C_2

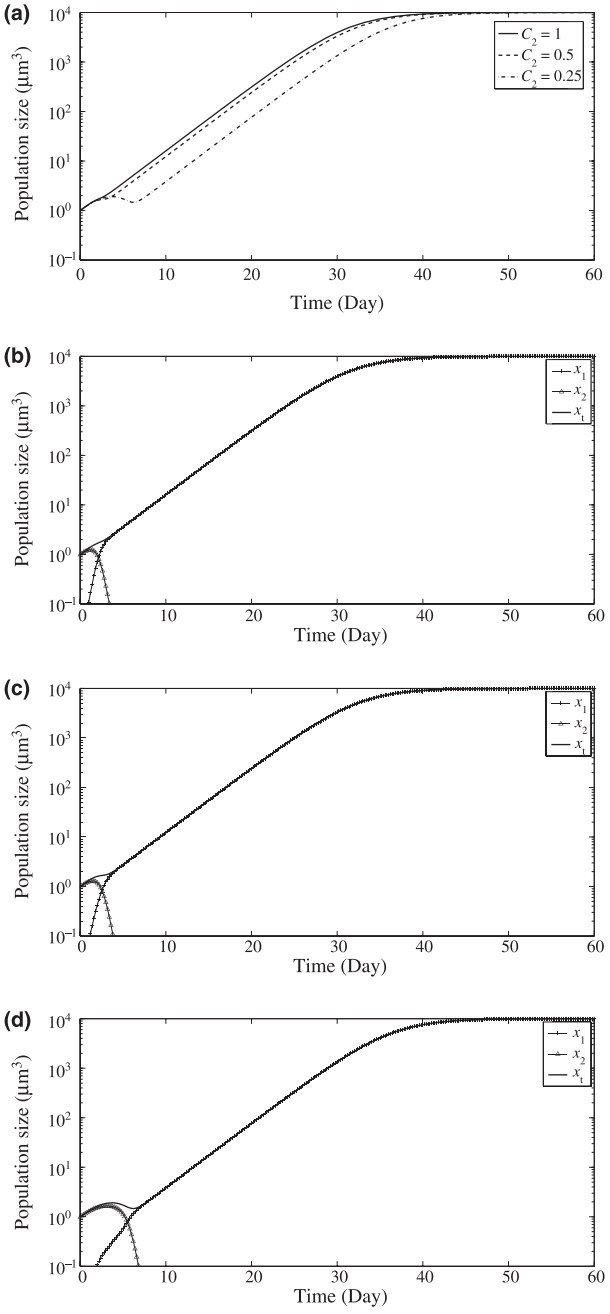

Figure 3. An illustration that the regulation of suppressing capacity C_2 can exhibit the delay feature. Growth curves with fixed system parameters and initial conditions (r = 0.3, $a = 10^6$, $C_1 = 10^4$, k = 2.5, $x_t(0)$ = 1, $w_1(0)$ = 0.01), but different C_2. (a) x_t for C_2 = 1 (solid), C_2 = 0.5 (dashed) and C_2 = 0.25 (dash-dot). As C_2 becomes smaller, a delayed phase becomes obvious. (b), (c) and (d) are growth curves of x_1, x_2, and x_t with different C_2. (b) C_2 = 1, (c) C_2 = 0.5, and (d) C_2 = 0.25, for x_t (bold), x_1 (marked with '+'), and x_2 (marked with 'Δ'). When C_2 is small, the inhibiting effects due to final dominant state x_1, is more pronounced during transience, and a delayed phase persists until x_2 becomes negligible (note that the ordinate is in logarithmic scale).

seemed to have a power law relationship. With this in mind, we tentatively choose treatment function $C_2 = 19.2 \times M^{0.6}$, where M is dose concentration of 17AAG in nM. As we have no access to the experimental value of w_1, we simply have to make an educated guess. Now that we are assuming that the effect of 17AAG is to inhibit population of x_1, we can hypothesize that the initial weighting w_1 is small. To be specific, we have taken the initial weighting w_1 of carcinoma spheroids treated with 17AAG to be $w_1(0) = 0.01$. Figure 4 shows the comparison between numerical results of our simulation concerning17AAG treatment and the actual experimental data. We have used Fig. 1 of Ref. (14) to extract data and plot them in juxtaposition with our fit. In Fig. 4a are shown the numerical fit (curves) and experimental data of 17AAG treatment (markers). Apparent in this figure is that the numerical fit works best in the high-dose regime, whereas the general trend is still captured in the low-dose regime. As good as the numerical fit may be, we must quickly point out that the merit of the present work does not lie in the good fit of the numerical values, but rather in the *qualitative* features it is capable of explaining, for the actual data. Once we know qualitatively what factors can affect treatment in which way, then a more refined model, surpassing the simple logistic growth considered here, presumably can be worked out to provide guidance (or even quantitative prediction) on how actual treatments should be carried out.

Shown in Fig. 4b are fitting parameter values versus dose concentration of 17AAG. Here, we see that C_2 changes more rapidly compared to other parameters when we vary concentration of 17AAG. This suggests that C_2 is probably the most relevant parameter when concentration of 17AAG is varied.

Irradiation

Irradiation is also a common treatment for cancer, although the underlying mechanism for its success seems to be complex. By observing growth curves with different doses of irradiation (14), we hypothesize that treatment by irradiation might reduce the value of the heterogeneity coefficient a and autocrine transition effect from x_2 to x_1. With this hypothesis in mind, we also evolved tentative treatment functions of irradiation for system parameters a and k. Let D denote dose/strength of irradiation in units Gy; treatment functions are taken to be $a = 10^{\frac{6}{D}-2}$ and $k = 2.5 - \frac{D}{2}$ respectively. As the heterogeneity coefficient is reduced under irradiation, it may imply that the original proliferating subpopulation x_2 is damaged more by irradiation. Hence, we think that initial weighting of w_1 may be closer to 1. In our simulation, we set the initial weighting to be $w_1(0) = 0.99$ (Fig. 5). Figure 6 shows our simula-

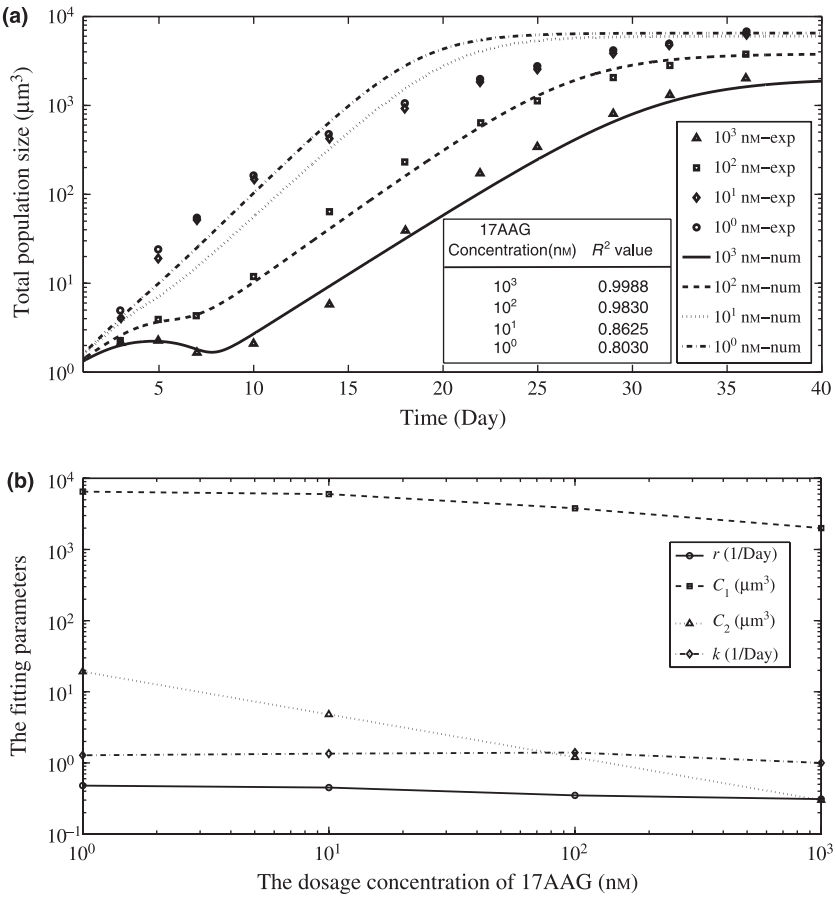

Figure 4. Fitting x_t growth curves with data from 17AAG treatment of Ref. (14). (a) numerical results (curves) compared to actual experimental data (markers). R^2 values of them are $R^2_{1\text{nM}} = 0.8030$, $R^2_{10\text{nM}} = 0.8625$, $R^2_{100\text{nM}} = 0.9830$ and $R^2_{1000\text{nM}} = 0.9988$. The fit is best in the high-dosage regime. (b) fitting parameters used in (a) as function of corresponding dosage.

tion results for irradiation. Notable features captured here are presence of a delayed phase at 6 Gy and inhibition of x_t size at 9 and 12 Gy, respectively, which correspond to Fig. 2 of Ref. (14).

Bi-stable behaviour

It is interesting to note that dependence of bi-stable behaviour on initial conditions has also been shown in actual tumour growth data [see Fig. 6a of Ref. (14)]. At 6 Gy irradiation, tumour growth curves had different final states (alive or dead) when tumours had different initial sizes. This seemed to correspond to existence of critical $x_t(0)$ in our model.

In comparison, Fig. 6a shows the numerical simulation of growth curves with different initial $x_t(0)$ in 6 Gy treatment. For easier comparison, we have also extracted data of Ref. (14) and reproduced them in Fig. 6b. Here, we see that the behaviour of the growth curve has a drastic change when $x_t(0) > 0.6$. In fact, this

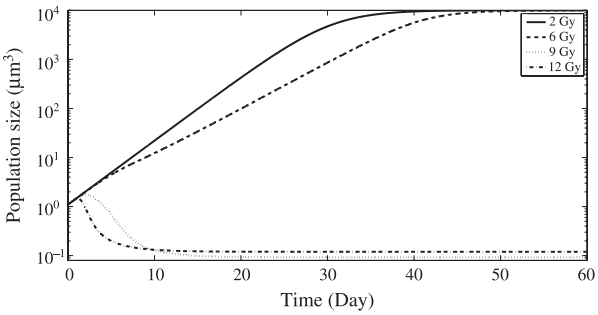

Figure 5. Fitting x_t growth curves of data from irradiation treatment. The system parameters are taken as ($r = 0.3$, $C_1 = 10^4$, $C_2 = 2$, $x_t(0) = 1.1$, $w_1(0) = 0.99$). Fitted x_t is for 2 Gy irradiation treatment (solid, $a = 10$, $k = 1.5$), 6 Gy irradiation treatment (dashed, $a = 0.1$, $k = -0.5$), 9 Gy irradiation treatment (dotted, $a = 0.0464$, $k = -2$) and 12 Gy irradiation treatment (dash-dot, $a = 0.0316$, $k = -3.5$). The fit compares favourably well with Fig. 2 of Ref. (14).

is because the initial value has crossed the critical value. Again, the simulation results shown in the bi-stable growth curves of Fig. 6a compare favourably well with

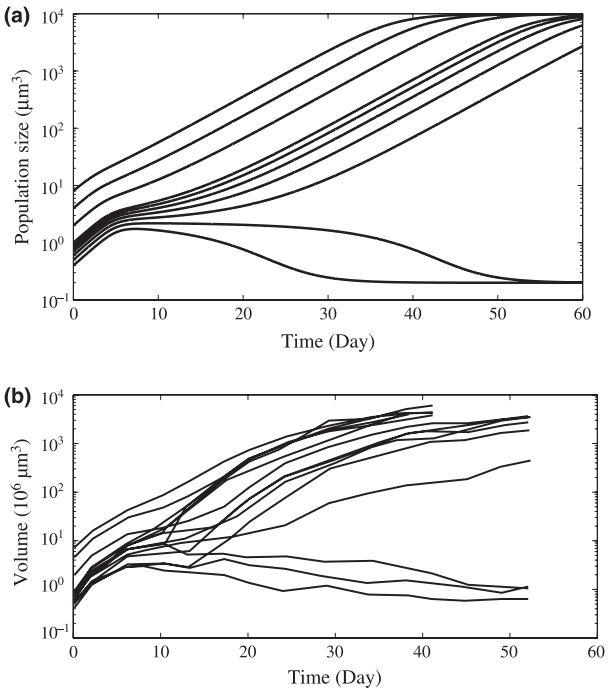

Figure 6. The comparison of the bi-stable behavior of the numerical result and the real data of 6Gy treatment. (a) Fitting x_t growth curve data near 6 Gy irradiation treatment, using the bi-stable model with different $x_t(0)$. The system parameters are taken as ($r = 0.3$, $a = 0.1$, $C_1 = 10^4$, $C_2 = 2$, $k = -0.8$, $w_1(0) = 0.99$). (a) corresponds well with data of 6 Gy treatment in prostate carcinoma spheroids (14). (b) Actual experimental data extracted from (a) of Ref. (14).

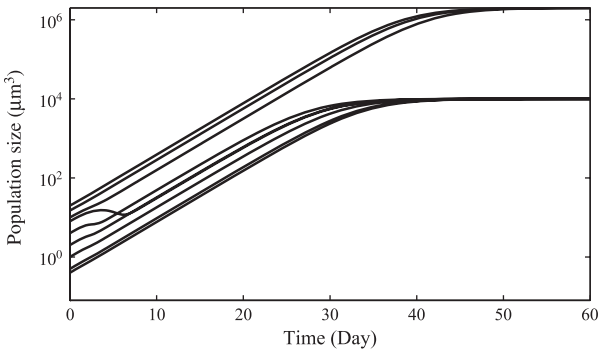

Figure 7. The numerical result of simulating the bi-stable behavior of 17AAG treatment. Fitting x_t growth curves of 1000 nM 17AAG treatment with different $x_t(0)$, using the bi-stable model. System parameters taken as ($r = 0.3$, $a = 10^6$, $C_1 = 10^4$, $C_2 = 2$, $k = 2.5$, $w_1(0) = 0.01$).

those in the actual 6 Gy treatment in prostate carcinoma spheroids (Fig. 6b).

Finally, another bi-stable figure when $a >> 1$ is also shown in Fig. 7. This also captures bi-stable behaviour for the growth curves with different initial total size x_t for the 1000 nM 17AAG treatment [See Fig. 6b of Ref. (14)].

Conclusion

A mathematical tumour growth model has the merit of helping us to single out potential effects of medical treatments on cancer growth and pointing out possible directions for improvement. Our heterogeneity cancer system model has been developed with this in mind. Although simplistic in nature, it seems to have captured some of the more pronounced features observed in actual cancer treatment. Specifically, our model shows that C_2, suppressing capacity of the cancer stem cell state, on the normal cancer cell state, can help explain presence of the delayed phase in actual treatment, whereas combination of the autocrine signalling pathway strength k and heterogeneity coefficient a, can regulate the final dominant state or exhibit a bi-stable phenomenon. For the latter to occur, initial conditions are shown to play an essential role as well. Our model seems to compare favourably with experimental data of Ref. (14), which deals with treatment of prostate carcinoma spheroids. Taken together, our study points out possible correlations between cancer treatments and our system parameters, each of which also admits a simple interpretation. We think that further study along this line might give us insight and guidance for future cancer research.

Acknowledgements

This work is supported in part by the National Science Council of the Republic of China under Grants No. NSC 100-2112-M-002-007 and NSC 100-2112-M-032-002-MY3, and the National Center for Theoretical Sciences in Taipei.

References

1 Reya T, Morrison SJ, Clarke MF, Weissman IL (2001) Stem cells, cancer, and cancer stem cells. *Nature* **414**, 105–111.
2 Gupta PB, Chaffer CL, Weinberg RA (2009) Cancer stem cells mirage or reality? *Nat. Med.* **15**, 1010–1012.
3 Grivennikov S, Karin M (2008) Autocrine IL-6 signaling: a key event in tumorigenesis? *Cancer Cell* **13**, 7–9.
4 Wolkenhauer O, Auffray C, Baltrusch S, Blüthgen N, Byrne H, Cascante M *et al.*2010) Systems biologists seek fuller integration of systems biology approaches in new cancer research programs. *Cancer Res.* **70**, 12–13.
5 Piotrowska MJ, Enderling H, An der Heiden U, Mackey MC (2008) Cancer and stem cells, chapter 2, New York: Nova Science Publishers, Inc.
6 Garner AL, Lau YY, Jordan DW, Uhler MD, Gilgenbach RM (2006) Implications of a simple mathematical model to cancer cell population dynamics. *Cell Prolif.* **39**, 15–28.
7 Ganguly R, Puri IK (2006) Mathematical model for the cancer stem cell hypothesis. *Cell Prolif.* **39**, 3–14.
8 Bajzer Ž, Vuk-Pavlović S (2005) Modeling positive regulatory feedbacks in cell–cell interactions. *Biosystems* **80**, 1–10.

9 Ghosh S, Elankumaran S, Puri IK (2011) Mathematical model of the role of intercellular signalling in intercellular cooperation during tumorigenesis. *Cell Prolif.* **44**, 192–203.
10 Swierniak A, Kimmel M, Smieja J (2009) Mathematical modeling as a tool for planning anticancer therapy. *Eur. J. Pharmacol.* **625**, 108–121.
11 Tanaka G, Hirata Y, Goldenberg SL, Bruchovsky N, Aihara K (2010) Mathematical modelling of prostate cancer growth and its application to hormone therapy. *Philos. Trans. R. Soc. A Math. Phys. Eng. Sci.* **368**, 5029–5044.
12 Leder K, Holland EC, Michor F (2010) The therapeutic implications of plasticity of the cancer stem cell phenotype. *PLoS One* **5**, e14366.
13 Ganguly R, Puri IK (2007) Mathematical model for chemotherapeutic drug efficacy in arresting tumour growth based on the cancer stem cell hypothesis. *Cell Prolif.* **40**, 338–354.
14 Enmon R, Yang WH, Ballangrud AM, Solit DB, Heller G, Rosen N *et al.* (2003) Combination treatment with 17-N-allylamino-17-demethoxy geldanamycin and acute irradiation produces supra-additive growth suppression in human prostate carcinoma spheroids. *Cancer Res.* **63**, 8393–8399.
15 Chang HH, Hemberg M, Barahona M, Ingber DE, Huang S (2008) Transcriptome-wide noise controls lineage choice in mammalian progenitor cells. *Nature* **453**, 544–548.
16 Usmani SZ, Bona R, Li ZH (2009) 17 AAG for HSP90 inhibition in cancer – from bench to bedside. *Curr. Mol. Med.* **9**, 654–664.

Appendix A: Transforming variables from (x_1, x_2) to (x_t, w_1)

$$\dot{x}_t = \dot{x}_1 + \dot{x}_2$$

$$= rx_1 + rx_2 - r\left(\frac{x_1}{C_1} + \frac{x_2}{C_2}\right)x_1 - \frac{r}{a}\left(\frac{x_1}{C_1} + \frac{x_2}{C_2}\right)x_2$$

$$= rx_t\left(1 - \left(\left(1 - \frac{1}{a}\right)w_1 + \frac{1}{a}\right)\left(\left(\frac{1}{C_1} - \frac{1}{C_2}\right)w_1 + \frac{1}{C_2}\right)x_t\right)$$

And form of $\dot{w}_1$ is

$$\dot{w}_1 = \frac{1}{x_t}(\dot{x}_1 - w_1\dot{x}_t)$$

$$= \frac{\dot{x}_1}{x_t} - w_1\frac{\dot{x}_t}{x_t}$$

$$= \left(k - r\left(1 - \frac{1}{a}\right)\left(\frac{w_1}{C_1} + \frac{1 - w_1}{C_2}\right)x_t\right)(w_1 - w_1^2).$$

Therefore,

$$\begin{cases} \dot{x}_t = rx_t\left(1 - \left[\left(w_1 + \frac{1-w_1}{a}\right)\left(\frac{w_1}{C_1} + \frac{1-w_1}{C_2}\right)\right]x_t\right), \\ \dot{w}_1 = k\left\{1 - \frac{r}{k}\left(1 - \frac{1}{a}\right)\left(\frac{w_1}{C_1} + \frac{1-w_1}{C_2}\right)x_t\right\}(w_1 - w_1^2). \end{cases} \quad \text{(A1)}$$

Notice that $\dot{x}_t$ is still of logistic growth form, but its associated self-suppressing capacity (all terms inside the square brackets) now is related to w_1. It is to be noted that $\dot{w}_1$ is also in logistic growth form, except that growth rate (all terms inside curly brackets) is modulated by w_1 and x_t. This view turns out to be helpful later when we discuss the time evolution of the system.

Appendix B: Nullcline equations

Nullclines are used to investigate when a variable of a dynamical system varies slowly in time. For instance, the nullcline equation of x_t (or w_1) is determined by requiring $\dot{x}_t = 0$ (or $\dot{w}_1 = 0$). With

$$\dot{x}_t = rx_t\left(1 - \left(\left(1 - \frac{1}{a}\right)w_1 + \frac{1}{a}\right)\left(\left(\frac{1}{C_1} - \frac{1}{C_2}\right)w_1 + \frac{1}{C_2}\right)x_t\right)$$

we can solve for the nullcline as

$$\tilde{x}_t = \frac{aC_2}{((a-1)\tilde{w}_1 + 1)((C_2/C_1 - 1)\tilde{w}_1 + 1)}, \quad \text{(B1)}$$

which is U-shaped when $\tilde{w}_1$ is chosen to be the abscissa. When we plot $\tilde{x}_t$ as a function of $\tilde{w}_1$, it can be easily checked that $\tilde{x}_t$ attains an extremely small value of $\frac{aC_2}{4}\left(\frac{1}{(a-1)(1-C_2/C_1)}\left(\frac{1}{1-C_2/C_1} + \frac{1}{a-1}\right)^2\right)$ at $\tilde{w}_1 = \frac{1}{2}\left(\frac{1}{1-a} + \frac{1}{1-C_2/C_1}\right)$ for the parameter regime we have adopted, namely, $C_1 >> C_2$ and $a >> 1$. In fact, the minimum is about $\frac{C_2}{4}$, with a corresponding $\tilde{w}_1 \sim 0.5$. This implies that when the percentage w_1 of state 1 gets near the value of this particular $\tilde{w}_1$, it is possible for total population to be varying slowly in time, provided x_t is simultaneously assuming a small value close to the lowest possible value given by eqn B1. Then, growth of total population comes to stagnation, and things change slowly in time, with the population having plunged into a dip. In other words, the system is exhibiting a delayed growth phenomena. In our model, this feature is used to provide qualitative as well as quantitative explanation of the experimental data. (For a more dynamical view, see the next section.)

We can also solve for the nullcline equation of w_1 by setting $\dot{w}_1 = 0$ in

$$\dot{w}_1 = \left(k - r\left(1 - \frac{1}{a}\right)\left(\left(\frac{1}{C_1} - \frac{1}{C_2}\right)w_1 + \frac{1}{C_2}\right)x_t\right)(w_1 - w_1^2).$$

Results are

$$\tilde{w}_1 = \begin{cases} 0 \\ 1 \end{cases},$$

or

$$\tilde{x}_t = \frac{k}{r(1 - \frac{1}{a})((\frac{1}{C_1} - \frac{1}{C_2})\tilde{w}_1 + \frac{1}{C_2})}. \quad \text{(B2)}$$

For parameter regime we have chosen, $\tilde{x}_t \approx \frac{C_2 k}{r(1-\tilde{w}_1)}$.

Appendix C: Bi-stable condition

In this system, we can easily find two trivial fixed points. They correspond to the final dominant state being either cancer stem cell state or normal cancer cell state. Mathematically, they are, $(x_t, w_1) = (C_1, 1)$ and $(x_t, w_1) = (aC_2, 0)$. Linear stability analysis about the first fixed point shows that it is stable when $kr\left(1 - \frac{1}{a}\right)$. Similar analysis shows that the second fixed point is stable when $kr(a-1)$. Since we always have $(a-1) \geq \left(1 - \frac{1}{a}\right)$, we conclude that

$$\begin{cases} \text{Only } (x_t, w_1) = (C_1, 1) \text{ is stable for } kr(a-1), \\ \text{Both } (C_1, 1) \text{ and } (aC_2, 0) \text{ are stable for } r(a-1)kr\left(1 - \frac{1}{a}\right), \\ \text{Only } (x_t, w_1) = (aC_2, 0) \text{ is stable for } kr\left(1 - \frac{1}{a}\right). \end{cases}$$

The above classification can be qualitatively understood in the following way: if the autocrine transition effect is 'turned off', that is, $k = 0$, then eqn 2 immediately tells us that, all things being equal, the second state experiences a lesser inhibiting effect from the two parameters C_1 and C_2, as $a > 1$ by our construction. Therefore, state 2 is expected to eventually dominate the population.

But if we increase the value of k, which means state 2 is converting part of its population to state 1 but not the other way around, then state 1 has an extra mechanism to increase its population at the expense of state 2. Thus, for an intermediate value of k, when competition and inhibition between the two states are comparable, initial conditions play an essential role in determining which is going to eventually dominate the scene, and we have a bi-stable scenario.

And when k becomes really large, state 2 tends to quickly convert itself into state 1 whenever it is generated, and so the final state is dominated by state 1.

The bi-stable scenario discussed above is also supported by simple mathematical analysis: It implies that, for the indicated parameter regime, there should exist another fixed point, which itself is unstable (so that it can drive the system to the two stable fixed points). Indeed, this extra fixed point can be found by combining the two nullcline equations eqns B1 and B2. Simple algebra leads to

$$\tilde{w}_1 = \frac{r}{k} - \frac{1}{a-1}.$$

As $\tilde{w}_1$ must lie between 0 and 1, we quickly derive the following condition: bi-stable conditions prevail when $r\left(1 - \frac{1}{a}\right)k(a-1)r$. This, of course, agrees with the argument above.

Appendix D: Simple analysis of time evolution of the system

With the assumption that $a >> 1$, the governing equation for x_2 takes an especially simple form

$$\dot{x}_2 \approx (r - kw_1)x_2,$$

whereas the equation for x_t is approximated by

$$\dot{x}_t \approx rx_t\left(1 - w_1\left(\frac{w_1}{C_1} + \frac{1 - w_1}{C_2}\right)x_t\right).$$

In view of the assumption that $C_1 >> C_2$, one may be tempted to also drop the term w_1/C_1 as well. However, this extra approximation may *not* be legitimate during the late stage of time evolution if state 1 dominates the final scene, as then $w_1 \approx 1$, which renders $(1 - w_1)/C_2$ small.

From the mathematical point of view, it is more convenient to de-dimensionalize the system. This can be done by the substitution

$$x_j \equiv x'_j C_1,\ x_t \equiv x'_t C_1$$

$$t \equiv rt',$$

$$k \equiv rk',$$

$$C' \equiv \frac{C_1}{C_2}.$$

The resulting equations then read

$$\frac{\mathrm{d}x'_2}{\mathrm{d}t'} \approx (1 - k'w_1)x'_2, \tag{D1}$$

$$\frac{\mathrm{d}x'_t}{\mathrm{d}t'} \approx x'_t\left[1 - w_1(w_1 + C'w_2)x'_t\right]. \tag{D2}$$

To provide a rough idea of orders of magnitude of the parameters we will be using, we list below their typical numerical values:

$$x'_1(0) \sim 10^{-6}, x'_2(0) \sim x'_t(0) \sim 10^{-4} so that w_1(0) \sim 10^{-2}$$

,

$$k' \sim 10, C' \sim 10^4$$

.

We now discuss time evolution of the system. To be specific, we will consider the case when state 1 is the minority at the beginning ($w_1 \approx 0$), but later gets to dominate the final stage *via* two mechanisms: the autocrine signalling pathway (assuming $k > 0$) in the early stage of time evolution, and the familiar logistic type growth. Total population x_t is also assumed small in the beginning.

The very early stage

With $w_1 \approx 0$ (species 1 being the minority) and $x_t \approx 0$, the governing equations are further simplified to

$$\frac{\mathrm{d}x_2'}{\mathrm{d}t'} \approx x_2',$$

$$\frac{\mathrm{d}x_t'}{\mathrm{d}t'} \approx x_t',$$

so that the two variables grow exponentially at about the same rate. However, we should *not* assume that x_1' behaves the same, because it is an even smaller quantity to begin with so that there is no telling directly from the two approximate equations above if $\dot{x}_1' = \dot{x}_t' - \dot{x}_2' \approx x_1'$. In fact, from eqn 2 we have

$$\begin{aligned}\frac{\mathrm{d}x_1'}{\mathrm{d}t'} &= \left[1 + k'w_2 - \left(x_1' + C'x_2'\right)\right]x_1' \\ &\approx \left[1 + k'w_2 - C'x_2'\right]x_1' \\ &\approx k'x_1'\end{aligned}$$

for the numerical values we have adopted. Hence, state 1 actually grows much faster than state 2 due to the autocrine transition effect, even though its population is only of the minority in the beginning.

With this in mind, and using a subscript 0 to denote the initial value, we see that

$$w_1 = \frac{x_1'}{x_t'} \approx \frac{x_{10}'}{x_{t0}'}\mathrm{e}^{(k'-1)t'},$$

which suggests that, by eqns D1 and D2, inhibition from w_1 on the growth of x_2 and x_t will quickly manifest itself as time proceeds.

The cross-over stage

When w_1 grows up to the order of $1/k'$, x_2' begins to feel the suppression in growth. The time τ_2' it takes for this to happen can be estimated *via*

$$\frac{x_{10}'}{x_{t0}'}\mathrm{e}^{(k'-1)\tau_2'} \sim \frac{1}{k'}$$

In contrast, for x_t' to begin experiencing any suppression in growth, we need a time τ_t' which can be estimated from solving

$$\begin{aligned}&w_1 \sim 1/C'x_2' \sim 1/C'x_t' \\ &\Rightarrow \frac{x_{10}'}{x_{t0}'}\mathrm{e}^{(k'-1)\tau_t'} \sim \frac{1}{C'x_{t0}'}\mathrm{e}^{-\tau_t'} \\ &\Rightarrow C'x_{10}'\mathrm{e}^{k'\tau_t'} \sim 1.\end{aligned}$$

For our choice of the parameters, it turns out that $\tau_t'\tau_2'$. This means that $(1 - k'w_1)$ in eqn D1 will become negative after a time of order τ_2', and so afterwards the growth of species 2 not only has been completely suppressed, but the autocrine transition is now actively converting virtually all of state 2 to state 1. In other words, the population of state 2 decreases rapidly afterwards.

If we denote the variables at the time when state 2 reaches its population maximum by an asterisk '*', then the scenario described above suggests expanding out $(1 - k'w_1) \approx -\alpha(t' - t'^*)$ for some number α so that, near this cross-over region, we have

$$\begin{aligned}&\frac{\mathrm{d}x_2'}{\mathrm{d}t'} \approx (1 - k'w_1)x_2' \approx -\alpha(t' - t'^*)x_2' \\ &\Rightarrow x_2' \approx x_2'^*\mathrm{e}^{-\alpha(t'-t'^*)^2/2}.\end{aligned}$$

Also, because $C'w_2w_1$ near the cross-over region, we may approximate eqn D2 as

$$\begin{aligned}\frac{\mathrm{d}x_t'}{\mathrm{d}t'} &\approx x_t'\left[1 - w_1(w_1 + C'w_2)x_t'\right] \\ &\approx x_t'\left[1 - w_1C'x_2'\right] \\ &\approx x_t'\left[1 - \left(\frac{1 + \alpha(t' - t'^*)}{k'}\right)C'x_2'\right].\end{aligned}$$

Hence, as t' increases from t'^* onward, x_t' reaches an extremum for time t'^* satisfying

$$0 = 1 - \left(\frac{1 + \alpha(t' - t'^*)}{k'}\right)C'x_2'.$$

For $t' - t'^*$ not too large, we may approximate the above by

$$\begin{aligned}0 &= 1 - \left(\frac{1 + \alpha(t' - t'^*)}{k'}\right)C'x_2'^*\mathrm{e}^{-\alpha(t'-t'^*)^2/2} \\ &\approx 1 - \left(\frac{1 + \alpha(t' - t'^*)}{k'}\right)C'x_2'^*\frac{1}{1 + \alpha(t' - t'^*)^2/2},\end{aligned}$$

which admits the following two solutions:

$$t' - t'^* = \frac{C'x_2'^*}{k'} \pm \sqrt{\left(\frac{C'x_2'^*}{k'}\right)^2 - \frac{2}{\alpha}\left(1 - \frac{C'x_2'^*}{k'}\right)}.$$

This means x_t' actually achieves a local maximum some time after state 2 reaches its maximum, then, as a result of the rapid decrease of state 2, the total population

plunges to a local minimum. It is only afterwards does the total population begin to pick up again, this time due to the logistic growth of the now-dominant species 1. Such a 'hiccup' is apparent in the numerical simulation of Fig. 3.

The late stage

Once the system has passed through the cross-over stage, the population of state 2 becomes negligible, and the time evolution of state 1 is basically that of the total population, which follows the simple logistic growth model, because

$$\frac{\mathrm{d}x'_t}{\mathrm{d}t'} \approx x'_t\left[1 - w_1(w_1 + C'w_2)x'_t\right]$$

$$\approx x'_t\left[1 - 1 \cdot (1 + C' \cdot 0)x'_t\right]$$

$$= x'_t\left[1 - x'_t\right].$$

This equation has the following solution:

$$x'_t \approx \frac{1}{1 - \left(1 - \frac{1}{x'_{t,h}}\right)\mathrm{e}^{-\left(t' - t'_h\right)}},$$

where a variable with the subscript 'h' means that it is evaluated at the time when the 'hiccup' in the total population ends.